CHAPTER III

RESULTS

3.1 Construction of a phagemid vector encoding scFv-M6-1B9

The heavy, Fd, and light chain domains of anti-CD147 mAb, M6-1B9 (Kasinrerk et al., 1999), were amplified, subcloned into the expression vector and then named as pCom3H-Fab-M6-1B9. Subsequently, the V_L and V_H were amplified from pCom3H-Fab-M6-1B9 and attached by a peptide linker to form the scFv. The amplified product was cloned into phagemid vector pComb3X, named pComb3X-scFv-M6-1B9, and then transformed into *E. coli* TG1. The nucleotide sequence of the inserted fragment, scFv, was obtained (**Figure 3.1**). The scFv construct was fused to the carboxy-terminal domain of the minor coat protein, gpIII, and displayed on the surface of phage particles. The deduced amino acid sequences of variable heavy (V_H) and light (V_L) chains are listed in **Figure 3.1.** The amino acid residues responsible for paratope in CDR regions were subsequently identified *via* the WAM (for Web antibody modelling) algorithm (Whitelegg and Rees, 2000). The sequence can be numbered following Kabat's rule (Kabat et al., 1976), in order to assure success in cloning the immunoglobulin variable domains.

```
                                                        SacI
  1 tgtgactggc tcgctacgtg gagaggcggc CGAGCTCgtg atgacccaga ctccagcact
    V   T   G   S   L   R   G   E   A   A   E   L   V   M*  T   Q   T   P   A   L
                                                        1>

 61 catggctgca tctccagggg agaaggtcac catcacctgc agtgtcagct caagtataag
 8>  M   A   A   S   P   G   E   K   V   T   I   T   C   S   V   S   S   S   I   S
                                                                        CDR1-V_L

121 ttccagcaac ttgcactggt accagcagaa gtcagaaacc tcccccaaac cctggattta
28>  S   S   N   L   H   W   Y   Q   Q   K   S   E   T   S   P   K   P   W   I   Y

181 tggcacatcc aacctggctt ctggagtccc tgttcgcttc agtggcagtg gatctgggac
48>  G   T   S   N   L   A   S   G   V   P   V   R   F   S   G   S   G   S   G   T
              CDR2-V_L

241 ctcttattct ctcacaatca gcagcatgga ggctgaagat gctgccactt attactgtca
68>  S   Y   S   L   T   I   S   S   M   E   A   E   D   A   A   T   Y   Y   C   Q

301 acagtggagt aattacccac tcacgttcgg tgctgggacc aagctggagc tgaaatcctc
88>  Q   W   S   N   Y   P   L   T   F   G   A   G   T   K   L   E   L   K   S   S
              CDR3-V_L
    ———————————————————— Linker peptide ——————————— XbaI
361 tggtggcggt ggctcgggcg gtggtggagg tggttccTCT AGAtcttccc tcgaggtaaa
108> G   G   G   G   S   G   G   G   G   G   S   S   R   S   S   L   E   V   K

            XhoI
421 gcttCTCGAG tctggggggag gcttagtgaa gcctggaggg tccctgaaac tctcctgtgc
128> L   L   E   S   G   G   G   L   V   K   P   G   G   S   L   K   L   S   C   A

481 agcctctgga ttcactttca gtagctatgc catgtcttgg gttcgccaga ctccggagaa
148> A   S   G   F   T   F   S   S   Y   A   M   S   W   V   R   Q   T   P   E   K
                          CDR1-V_H

541 gaggctggag tgggtcgcaa ccattagtag tggtggtact tacacctact atccagacag
168> R   L   E   W   V   A   T   I   S   S   G   G   T   Y   T   Y   Y   P   D   S
                                                            CDR2-V_H

601 tgtgaagggt cgattcacca tctccagaga caatgccaag aacaccctgt acctgcaaat
188> V   K   G   R   F   T   I   S   R   D   N   A   K   N   T   L   Y   L   Q   M

661 gagcagtctg aggtctgagg atacggccat gtattactgt gcaagattcc gtaacggcgc
208> S   S   L   R   S   E   D   T   A   M   Y   Y   C   A   R   F   R   N   G   A
                                                            CDR3-V_H

721 ttactggggc caagggactc tggtcactgt ctctgcagct acaacaacag ccccatctgt
228> Y   W   G   Q   G   T   L   V   T   V   S   A   A   T   T   T   A   P   S   V

            SpeI           SfiI    ——— 6× His tag ———                  HA tag
781 cACTAGTggc caGGCCGGCC agCACCATCA CCATCACCAT ggcgcaTACC CGTACGACGT
248> T   S   G   Q   A   G   Q   H   H   H   H   H   H   G   A   Y   P   Y   D   V

841 TCCGGACTAC GCTtcttagg agggtggtgg ctctgagggt ggcggttctg agggtggcgg
268> P   D   Y   A   S   *
```

Figure 3.1 Nucleotide sequence of cDNA and deduced amino acid sequence of the scFv-M6-1B9. The cDNA sequence encoding scFv-M6-1B9 was shown. Restriction endonuclease sites, histidine tag, and HA tags are indicated. The deduced amino acid sequence of scFv-M6-1B9 corresponding to the complementary determining regions (CDRs) in the variable regions of the L (red letters) and H (green letters) chains, which were identified by the Kabat numbering scheme, are indicated by gray boxes. Amino acids were numbered from the initiator methionine (M*). The amber stop codon was shown by an asterisk (*). The details of the CDRs region of scFv-M6-1B9 are shown as CDR1-V_L C-(^{24}SV---LH^{35}) W, CDR2- V_L Y (^{51}GT---AS ^{57}) G, CDR3- V_L C (^{90}QQ---PL^{97}) T, CDR1- V_H S (^{153}GF---MS^{162})W, CDR2- V_H A(^{178}IS---KG^{193})R, and CDR3- V_H R (^{226}FR---GAY^{231})W.

3.2 Detection of phage-displayed scFv-M6-1B9

The expression of Fab- and scFv-M6-1B9 on phage particles was assessed by Western immunoblotting. Equal amounts of each recombinant phage were fractionated by SDS–PAGE, blotted, and investigated with anti-gpIII mAb. The immunoreactive bands of scFv-M6-1B9- and Fab-M6-1B9-gpIII fusion protein with the approximate molecular weight of 47 kDa were obtained (**Figure 3.2A**). The band corresponding to the scFv-gpIII fusion protein was more prominent than the band corresponding to the Fab-M6-1B9-gpIII fusion protein, reflecting the fact that scFv expression was superior to that of Fab obtained by the phage display technique. Antigen-specific binding of phage presenting the different antibody formats was verified by ELISA using recombinant CD147-BCCP as an antigen. scFv format demonstrated more favorable antigen-binding features than the Fab format (**Figure 3.2B**). In contrast, VCSM13 phage prepared from non-transformed TG-1 did not generate the signal against CD147-BCCP antigen. These results imply that phage presenting different antibody formats of M6-1B9 had been successfully produced and the scFv version was the better functional antibody fragment.
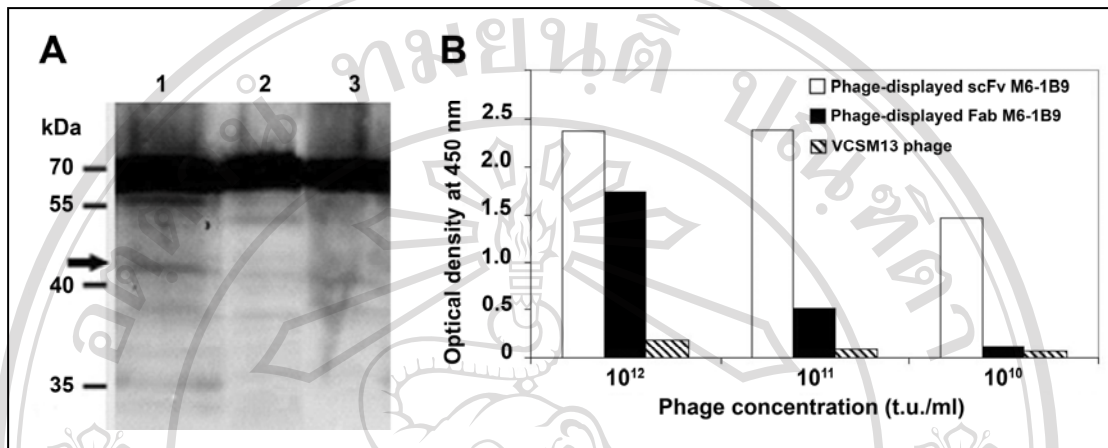
Figure 3.2 Verification of antibody phage presenting different formats.
(**A**) Recombinant phages (10^{13} t.u./lane) were separated on a reducing 12% SDS–PAGE. The gpIII protein was probed using anti-gpIII mAb. The immunoreactive bands were visualized by chemiluminescence substrate detection system. Lane 1, phage-displayed scFv-M6-1B9; lane 2, phage-displayed Fab-M6-1B9 and lane 3, VCSM13 helper phage. Molecular weight markers in kDa are indicated. (**B**) CD147-BCCP was captured on wells coated with avidin. Three different concentrations, 10^{10}-10^{12} t.u./ml of phage-displayed scFv-M6-1B9 and phage-displayed Fab-M6-1B9 were added and traced by peroxidase-conjugated anti-M13 phage mAb. VCSM13 helper phage was used as wild-type phage control.

3.3 Detection and characterization of soluble scFv-M6-1B9 produced in *E. coli*

The pComb3X-scFv-M6-1B9 was transformed into *E. coli* HB2151 to produce the soluble scFv antibody. The presence of soluble scFv in the culture supernatant was detected by Western immunoblotting using antibodies specific to the HA and His tags. The reactive bands revealed by anti-HA or anti-His were located at the same molecular weight (~30 kDa) (**Figure 3.3A**). This result indicates that soluble scFv-M6-1B9 was successfully produced by *E. coli* HB2151. The specificity of soluble scFv-M6-1B9 was analyzed by ELISA using CD147-BCCP as antigen. At least 1:100 dilution of soluble scFv-M6-1B9 has been shown the strongly positive signal with CD147-BCCP (**Figure 3.3B**). No signal was detected in the control well of SVV-BCCP antigen. Subsequently, the specificity of the generated scFv-M6-1B9 against recombinant CD147 was confirmed by Western immunoblotting. A specific band of CD147-BCCP at ~35 kDa was detected by probing with soluble scFv-M6-1B9 (**Figure 3.3C**). In addition, the native epitope of CD147 on the U937 cell surface was recognized by soluble scFv-M6-1B9 using flow cytometric analysis. The mean fluorescence intensity (MFI) of CD147 cell surface expression on U937 cells stained with soluble scFv-M6-1B9 was 10.42 (**Figure 3.3D**). This was similar to the value for the original antibody, M6-1B9, which MFI was 9.21 as shown in **Figure 3.3D**. These results strongly suggested that the generated soluble scFv-M6-1B9 carry a CD147-specific paratope which recognized both recombinant and native CD147.
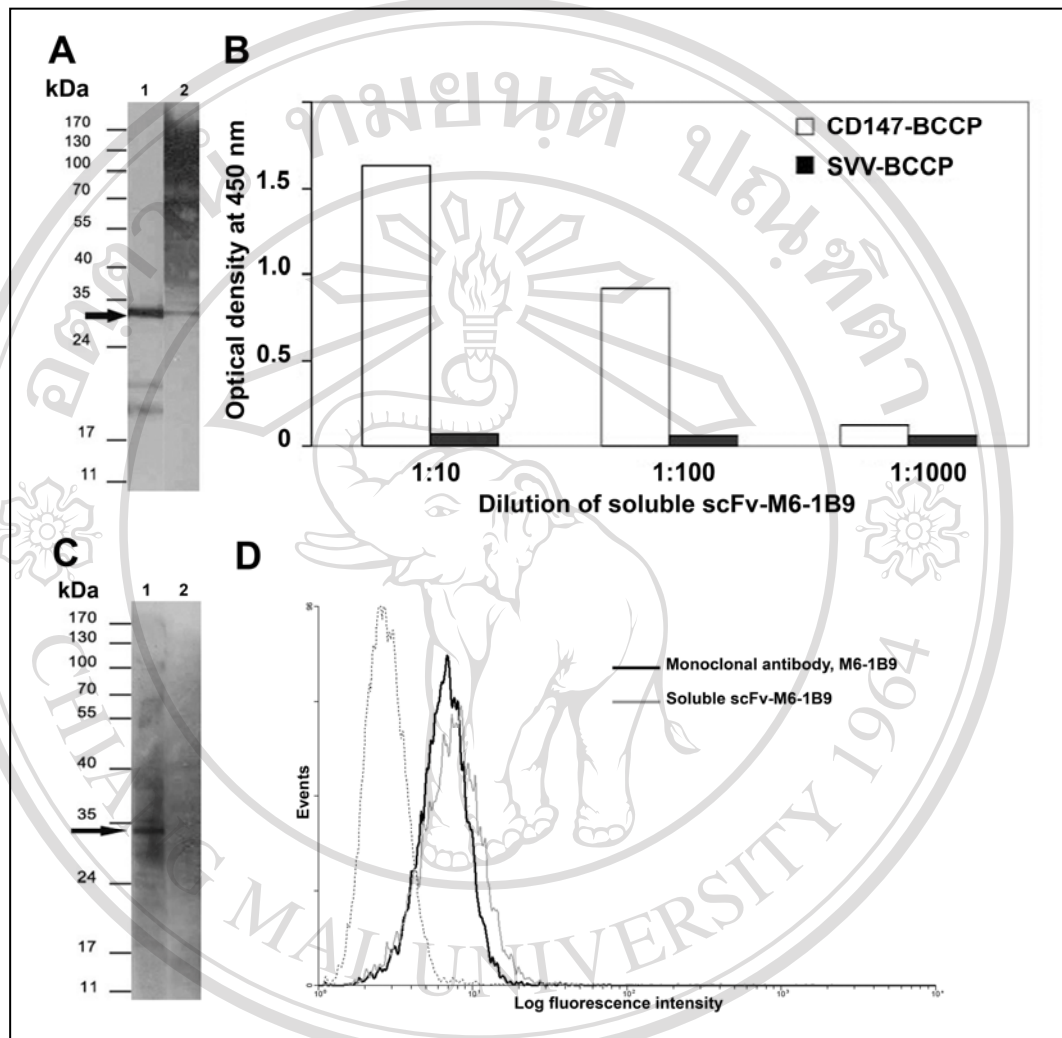
Figure 3.3 Detection of soluble scFv. (A) Soluble scFv-M6-1B9 was separated on 12% SDS-PAGE, electroblotted onto PVDF membrane, and probed with peroxidase-conjugated mAb anti-HA (lane 1) and anti-His mAb (lane 2). The immunoreactive bands were visualized by ECL substrate detection system. The molecular weight is indicated. **(B)** CD147-BCCP (open columns) or SVV-BCCP (black columns) was captured on the avidin-coated wells. Soluble scFv-M6-1B9 was subsequently added and the bound scFv was detected by peroxidase-conjugated mAb

anti-HA. **(C)** CD147-BCCP (lane 1) or SVV-BCCP (lane 2) proteins were separated on 12% SDS-PAGE, electroblotted onto a PVDF membrane, and then probed with soluble scFv-M6-1B9. The scFv was detected using peroxidase-conjugated mAb anti-HA. The positions of molecular mass markers are shown on the left. **(D)** CD147 on U937 cells was stained with soluble scFv-M6-1B9 and then probed by mouse anti-HA-biotin. Subsequently, FITC-conjugated sheep anti-mouse immunoglobulins antibody was added. Monoclonal antibody M6-1B9 was used as a control system for detecting CD147 on U937 cells. The immunofluorescence on cells stained with soluble scFv-M6-1B9 (bold line) or mAb M6-1B9 (thin line) is shown. The dashed line represents background fluorescence of negative control mAb. The y axis represents the number of events on a linear scale; the x axis shows the fluorescence intensity on a logarithmic scale.

To further characterize the specificity of the produced scFv, the inhibiting activity of soluble scFv-M6-1B9 with the original monoclonal antibody, M6-1B9, was tested. The optical density of mixture of soluble scFv-M6-1B9 and mAb M6-1B9 was lower than soluble scFv-M6-1B9 alone (**Figure 3.4**). In contrast, an irrelevant mAb (MT-SVV3) had no inhibitory effect on CD147 binding of soluble scFv-M6-1B9. This indicates that mAb M6-1B9 altered the binding of soluble scFv-M6-1B9 to recombinant CD147 and bound to the same epitope.
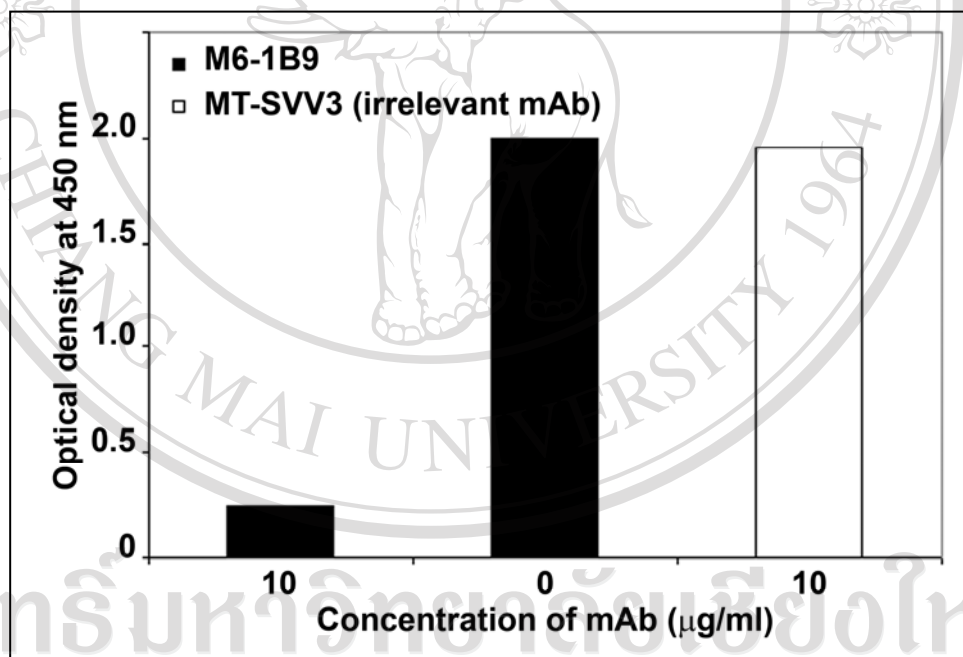
Figure 3.4 Competitive binding analysis of soluble scFv-M6-1B9 and mAb M61B9. CD147-BCCP was added onto avidin-coated wells. The mixture contained soluble scFv-M6-1B9 and mAb M6-1B9 at ratio 1:1 was added into the well. The bound scFv was detected by peroxidase-conjugated mAb anti-HA.

3.4 Soluble scFv-M6-1B9 inhibited CD3 mAb induced cell proliferation

To investigate the biological functions of soluble scFv-M6-1B9, the effect scFv-M6-1B9 on cell proliferation was assayed. PBMCs isolated from healthy donors were activated by immobilized CD3 mAb OKT3 in the presence or absence of CD147 mAb clone M6-1B9 or soluble scFv-M6-1B9. The results showed that soluble scFv-M6-1B9 inhibited colony formation (**Figure 3.5A**) and proliferation (**Figure 3.5B**) of PBMCs induced by CD3 mAb OKT3 as well as its original antibody (Chiampanichayakul et al., 2006). In contrast, mock bacterial protein lysate controls had no inhibitory effect on OKT3-mediated cell proliferation. These results demonstrate that the monomeric form of CD147 mAb could engage the CD147 molecule and induce negative regulation of OKT3-induced T cell proliferation. In addition, the results indicate that the produced soluble scFc-M6-1B9 is a biologically active protein.
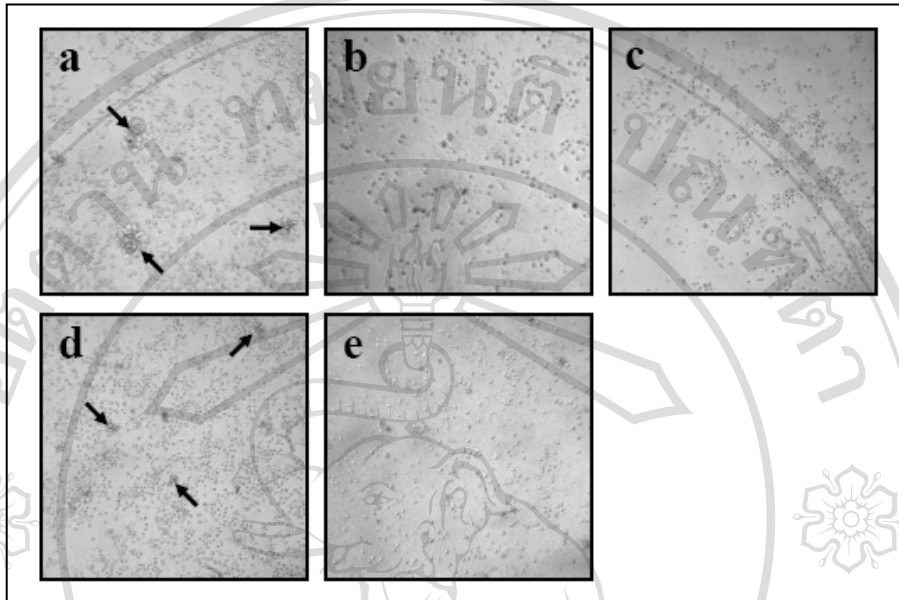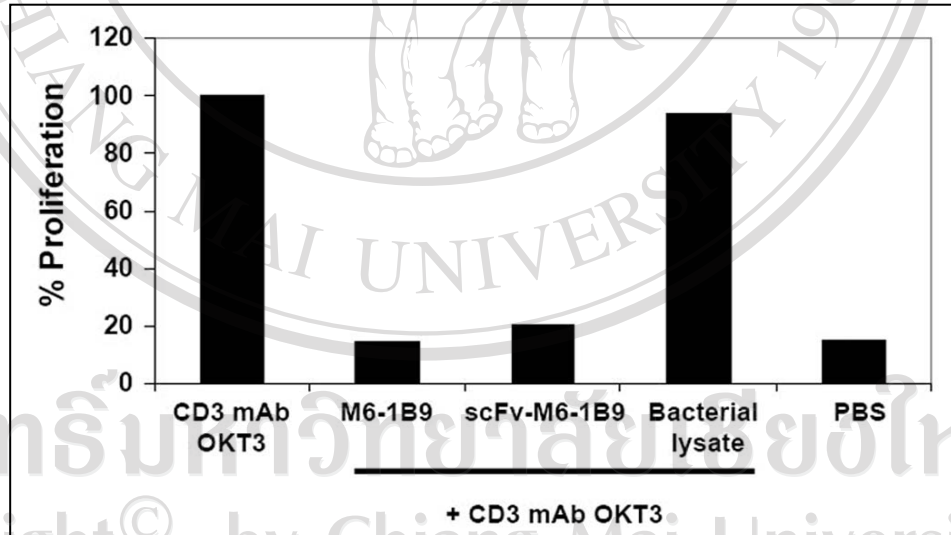
Figure 3.5 Soluble scFv-M6-1B9 inhibited CD3 mAb induced cell proliferation. (A) Photomicrography (100×) of colony formation of PBMC induced by CD3 mAb OKT3. Cells were stimulated with 20 ng/ml of immobilized CD3 mAb OKT3 in the presence or absence of CD147 mAb M6-1B9, scFv-M6-1B9 or bacterial protein lysate and observed under an inverted microscope. CD3 mAb OKT3 only (a),

CD3 mAb OKT3 plus M6-1B9 (20 μg/ml) (b), scFv-M6-1B9 (1:40) (c), bacterial protein lysate (1:40) (d), or PBS alone (e). Cell clustering is indicated by arrow. **(B)** Cell proliferation was determined by the measurement of CSFE incorporation using flow cytometry.
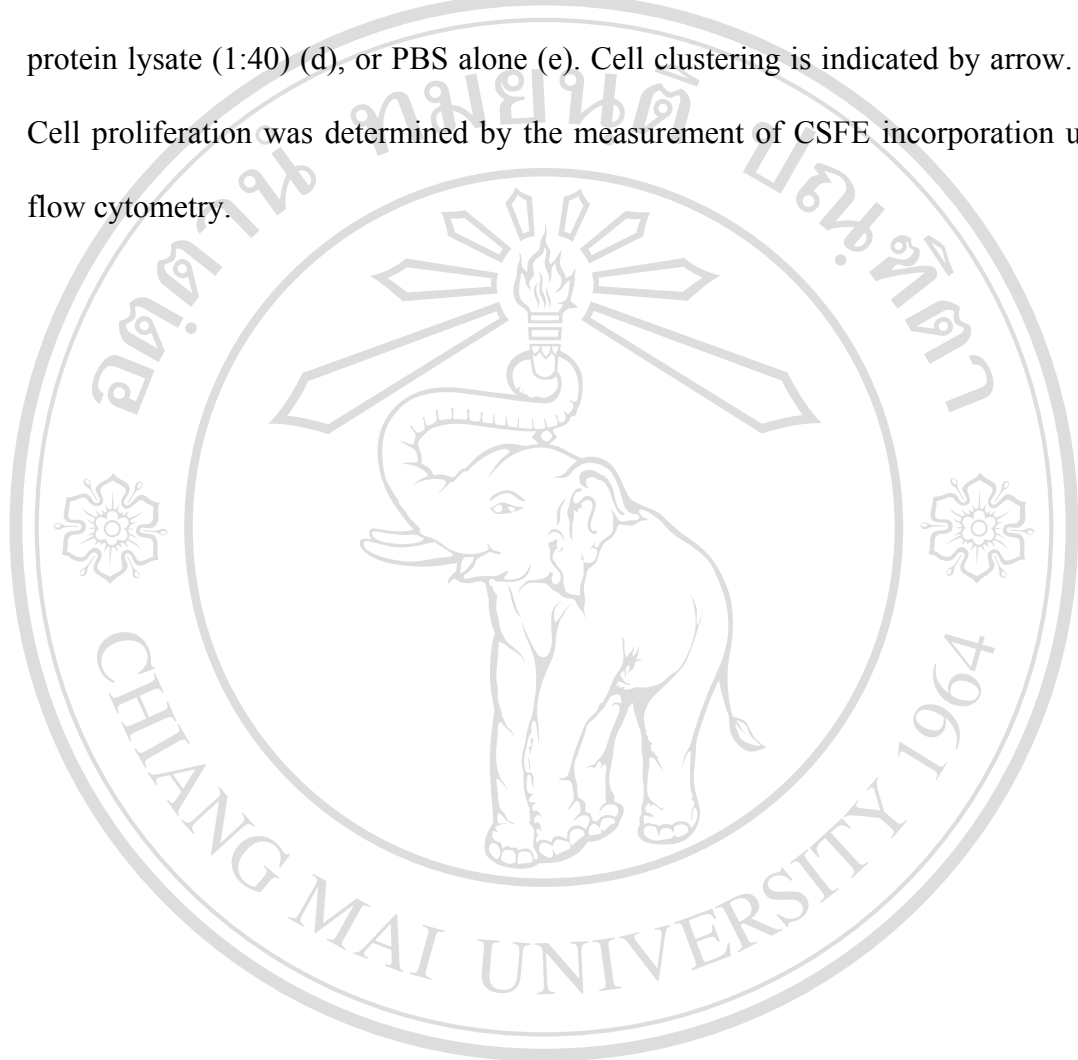
3.5 Generation of recombinant adenoviral vectors using the AdEasy method

To generate recombinant adenoviral vectors, *Pme*I linearized shuttle vector DNA (pAdT-scFv-M6-1B9) was co-transformed with supercoiled pAdEasy-1 plasmid into electrocompetent BJ5183 cells **(Figure 3.6A)**. Homologous recombinants were selected on LB plates containing 50 μg/ml kanamycin. Recombinant adenoviral vector was then extracted using Plasmid Mini Kit (QIAGEN). The corrected clone was analyzed by size and *Pac*I restriction mapping. Based on the migration rates, all clones were potential valid recombinants **(Figure 3.6B)**. Recombinants were generated by homologous recombination of the left and right arm sequences, but sometimes occurred between the plasmid *Ori* sequences shared between the shuttle and pAdEasy vector resulted in slightly different restriction patterns **(Figure 3.6C)**. Recombinant plasmids are propagated in a bacterial strain less prone to recombination than BJ5183, such as DH10B cells. Selected clones from DH10B cells were digested with *Pac*I restriction endonucleases to verify proper recombination. As shown in **Figure 3.6C**, a 3.0 kb (or 4.5 kb) fragment was produced when digested with *Pac*I.
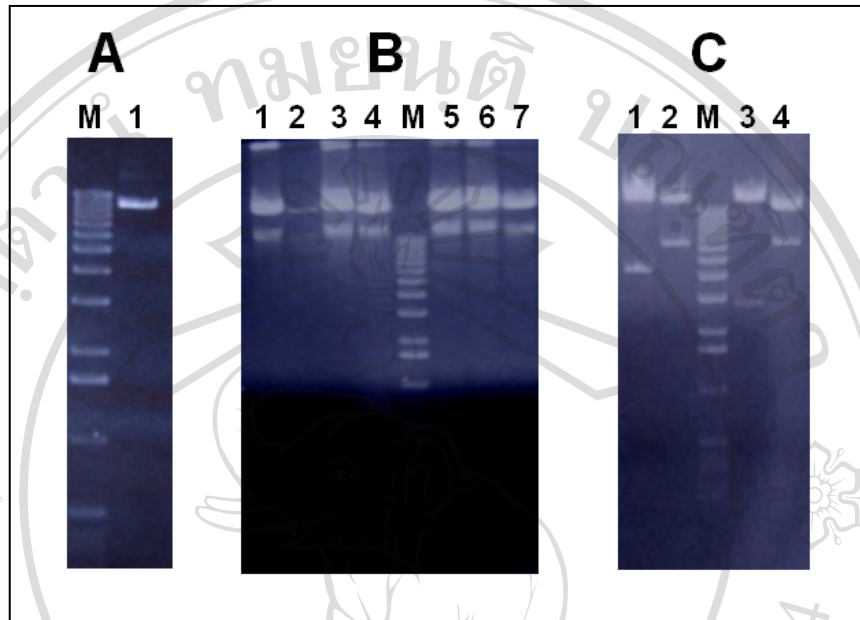
Figure 3.6 **Generation of recombinant adenoviral vectors in bacterial cells.** **(A)** pAdT-scFv-M6-1B9 was linearized with *Pme*I. **(B)** Recombinant pAdE-scFv-M6-1B9 (or pAdE/F35-scFv-M6-1B9) constructs derived from homologous recombination of pAdT-scFv-M6-1B9 and pAdEasy-1 (or pAdEasy-1/35) in BJ5183 cells were purified from minipreps. Lanes 1-4, four different pAdE-scFv-M6-1B9 clones, lanes 5-7, three different pAdE/F35-scFv-M6-1B9 clones and M, 1kb DNA marker. **(C)** Representative digestion with *Pac*I. Recombinant pAdE-scFv-M6-1B9 and pAdE/F35-scFv-M6-1B9 constructed from DH10B cells was purified from minipreps. Lanes 1 and 3, pAdE-scFv-M6-1B9 and pAdE/F35-scFv-M6-1B9 clones treated with *Pac*I, lanes 2 and 4, untreated *Pac*I and M, 1 kb DNA marker. The DNA was analyzed in supercoiled form by electrophoresis through an 0.8% agarose gel and ethidium bromide staining.

3.6 Generation of recombinant adenovirus expressing scFv-M61B9

The recombinant adenoviral plasmid vector (pAdE-scFv-M6-1B9 or pAdE/F35-scFv-M6-1B9) was linearized with *Pac*I to expose its inverted terminal repeats and transfected into a packaging cell line (293A) which constitutively expresses the E1 gene products required for the recombinant adenovirus propagation. The process of viral production can be followed in the packaging cells by visualization of the GFP reporter that is incorporated into the viral backbone (**Figure 3.7**). Comet-like adenovirus-producing foci became apparent at 5-7 days after transfection and plaques formation appeared at day 9-13. After 10–14 days, viruses were harvested, amplified by infecting packaging cells and purified by CsCl step gradients (**Figure 3.8**). The band containing parental full-length virus was carefully collected from each tube (**Figure 3.8A**), combined, and subjected to ultracentrifugation in an equilibrium gradient derived from 1.35 g/ml CsCl for 18 h at 14 °C and 35,000 rpm. The full-length band was collected again (**Figure 3.8B**) and dialyzed twice against 1 liter dialysis buffer at 4 °C in the dark for 6-8 h each. The virus is aliquoted and stored at –70 °C.
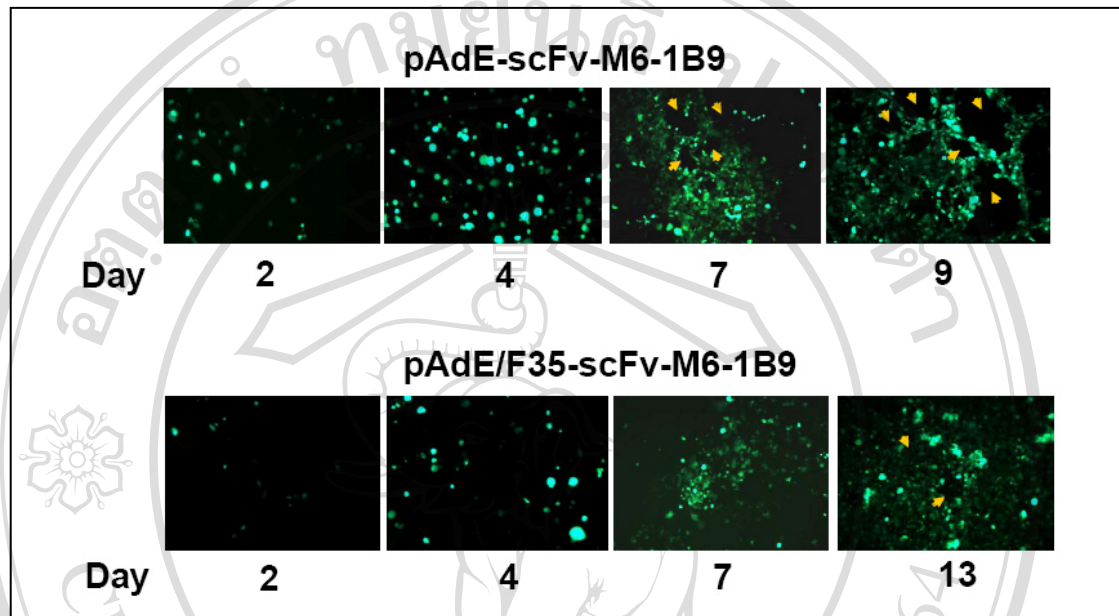
Figure 3.7 Adenovirus production after transfection of 293 cells. 293 cells were transfected with 5 μg of the *Pac*I digested pAdE-scFv-M6-1B9 (or pAd5/F35-scFv-M6-1B9) by transfection reagent. The transfected cells were monitored for GFP expression under fluorescence microscope at 100 × magnification.   Yellow arrow head showed plaques formation.
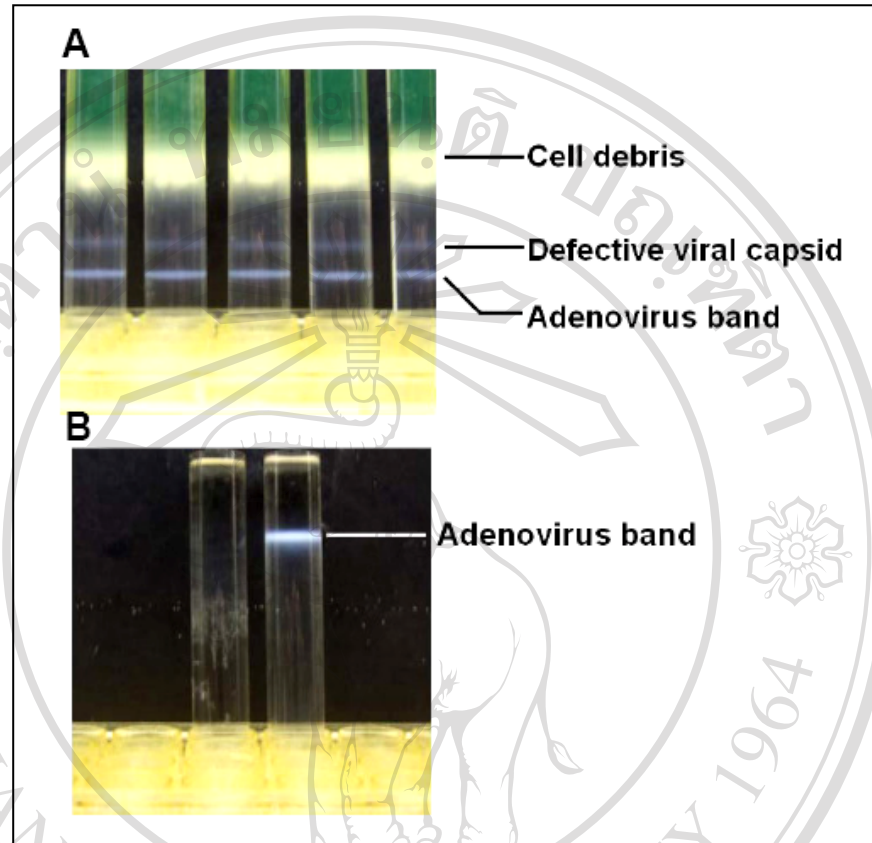
131

Figure 3.8 Adenovirus purification by CsCl step gradients. The band containing parental full-length virus was collected from ultracentrifuged tube. **(A)** first spinning and **(B)** second spinning.

3.7 Detection and characterization of scFv-M6-1B9 intrabody produced in 293A cells

To detect the presence of adenovirus knob, purified recombinant adenoviruses were employed for Ad5- and Ad35 knob amplification using specific primer sets. The result from polymerase chain reaction method showed a specific band at 220 bp. This result indicated that no cross contamination between recombinant Ad-scFv-M6-1B9 and Ad5/F35-scFv-M6-1B9 **(Figure 3.9)**.

A   **B**
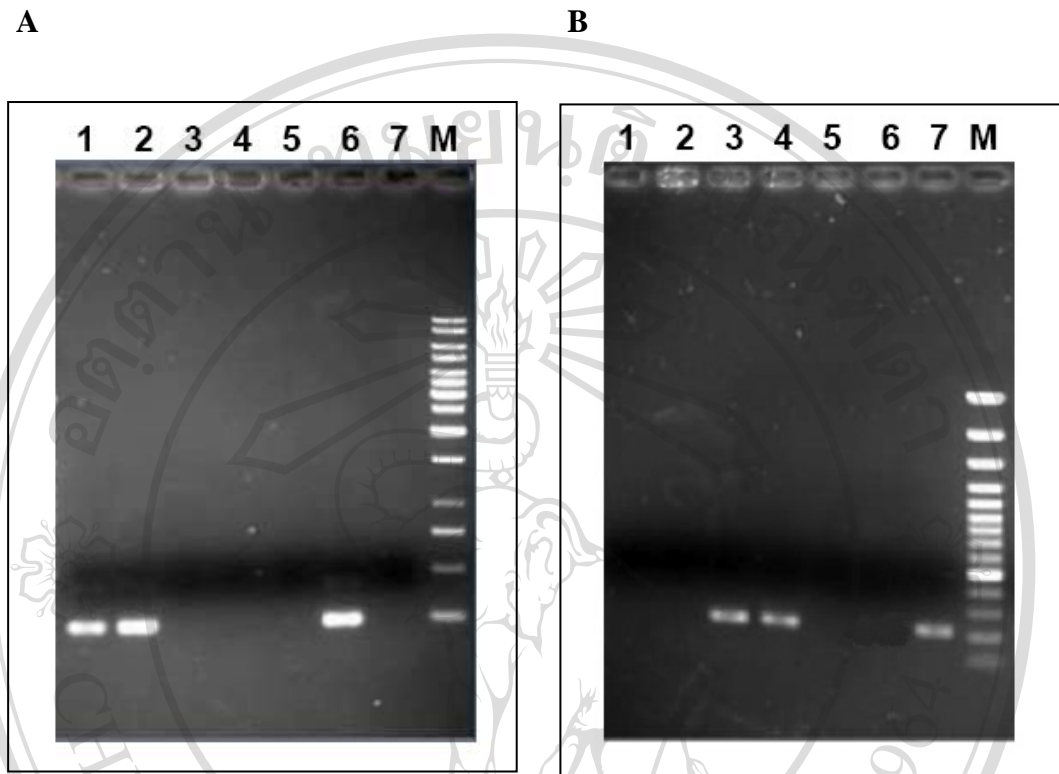
Figure 3.9 Adenovirus knob amplification. An equal amount of each adenovirus was amplified by PCR using Ad5 knob primers set **(A)** and Ad35 knob primer set **(B)**. Ad5-scFv-M6-1B9 (lane 1), Ad5-GFP (lane 2), Ad5/F35-scFv-M6-1B9 (lane 3), Ad5/F35-GFP (lane 4), negative control (lane 5), pAdE-scFv-M6-1B9 (lane 6) and pAdE/F35-scFv-M6-1B9 (lane 7) were used as a template. M indicated 1 kb DNA marker.

To confirm whether the recombinant adenovirus expressing scFv-M6-1B9, 293A cells were transduced with recombinant Ad-scFv-M6-1B9 (or Ad5/F35-scFv-M6-1B9) and harvested after 48 h. The lysate of transduced cells were separated on 12% SDS-PAGE and electroblotted onto a PVDF membrane. The presence of scFv-M6-1B9 intrabody in the cell lysate was detected by Western immunoblotting with an HA tag. The reactive band revealed by anti-HA was detected in the cell lysates from 293A transduced with both recombinant Ad-scFv-M6-1B9 and Ad5/F35-scFv-M6-1B9 (~35 kDa) and not found in the cell lysates from 293A transduced with recombinant Ad5-GFP, Ad5/F35-GFP and untransduced 293A cells (**Figure 3.10**). This result indicates that recombinant Ad-scFv-M6-1B9 and Ad5/F35-scFv-M6-1B9 was able to express a scFv-M6-1B9.
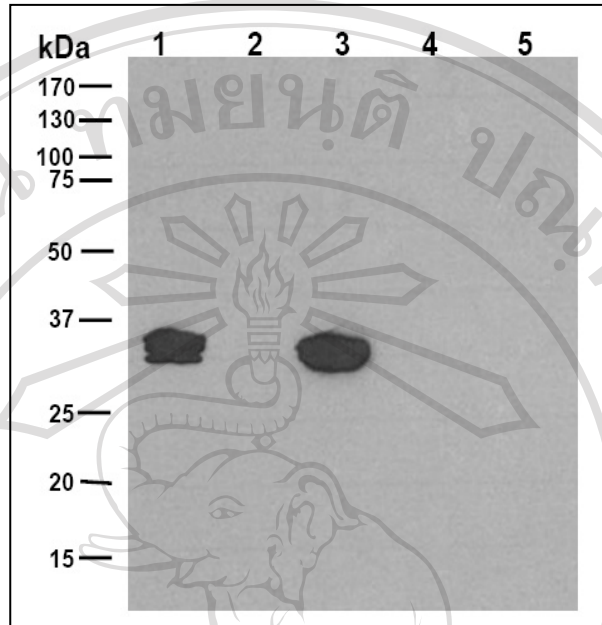
Figure 3.10 Detection of scFv-M6-1B9 intrabody expression by Western blotting. 293A cells were transduced with recombinant adenovirus harboring scFv-M6-1B9**.** Cells were lysated and separated on 12% SDS-PAGE, electroblotted onto a PVDF membrane. The produced scFv intrabody was detected using peroxidase-conjugated mAb anti-HA. The positions of molecular mass markers are shown on the left. The cell lysate obtained from Ad-scFv-M6-1B9 (lane 1), Ad5-GFP (lane2), Ad5/F35-scFv-M6-1B9 (lane 3), Ad5/F35-GFP (lane 4) transduced and untransduced 293A cells (lane 5) were indicated.

To further investigate the intracellular expression of scFv, the lysate fractions of transduced cells were separated on 12% SDS-PAGE and electroblotted onto a PVDF membrane. The presence of scFv-M6-1B9 intrabody in the fractionated cell lysate was detected in the endoplasmic reticulum fraction (~35 kDa) and not found in the nuclear and cytoplasmic fractions (**Figure 3.11A**). This result demonstrates that an intrabody with a carboxyl-terminal endoplasmic reticulum (ER) retention signal (KDEL) was retained in the ER compartment.

Subsequently, the specificity of scFv-M6-1B9 intrabody in cell lysate was analyzed by immunoblotting using CD147-BCCP as antigen (Tayapiwatana et al., 2006). A specific band of CD147-BCCP at ~35 kDa was detected by probing with soluble scFv-M6-1B9 intrabody (**Figure 3.11B**). As control, soluble scFv-M6-1B9 produced by non-suppressor *E. coli* strain HB2151 gave also a positive signal with CD147-BCCP. No signal was detected in the control panel of survivin-BCCP (SVV-BCCP) antigen and bacterial lysate proteins. This result indicates that a specific and active scFv-M6-1B9 intrabody was successfully produced inside the transduced 293A cells.
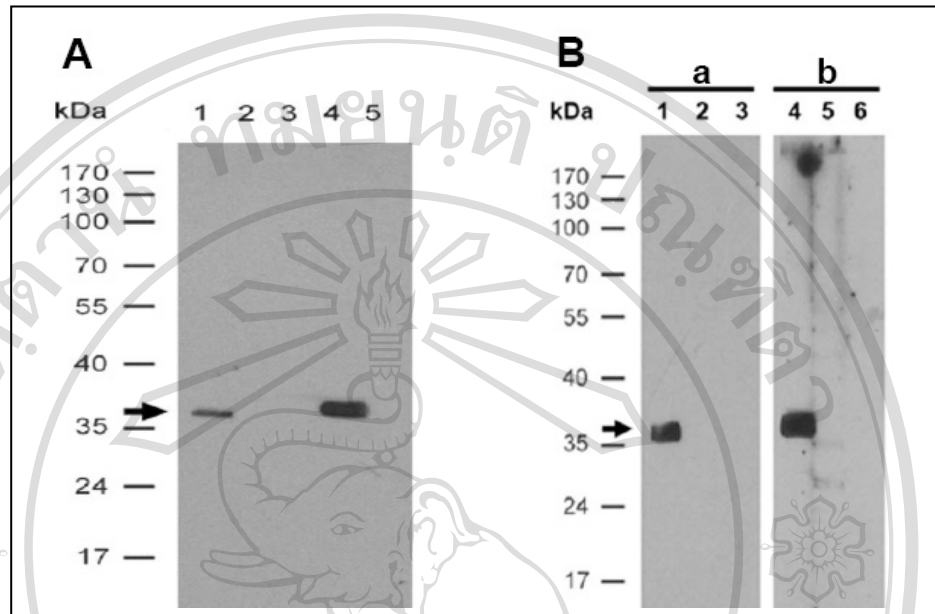
Figure 3.11 Detection of scFv-M6-1B9 intrabody activity by Western blotting. **(A)** 293A cells were transduced with recombinant adenovirus harboring scFv-M6-1B9. Cells were lysated and separated on 12% SDS-PAGE, electroblotted onto a PVDF membrane. The produced scFv intrabody was detected using peroxidase-conjugated mAb anti-HA. The positions of molecular mass markers are shown on the left. Soluble scFv-M6-1B9 produced by expressing pComb3X-scFv-M6-1B9 phagemid in the non-suppressor *E. coli* strain HB2151 was used as positive control (lane 1). Transduced 293A cell lysate obtained from nuclear fraction (lane 2), cytoplasmic fraction (lane 3), ER fraction (lane 4) and untransduced cells (lane 5) were indicated. **(B)** CD147-BCCP (lane 1, 4), SVV-BCCP (lane 2, 5) and bacterial lysate proteins (lane 3, 6) were separated on 12% SDS-PAGE, electroblotted onto a PVDF membrane, and then probed with M6-1B9 antibody (panel a) and soluble scFv-M6-1B9 intrabody (panel b). The M6-1B9 or scFv obtained from Ad-scFv-M6-1B9 transduced 293A cells was detected using peroxidase-conjugated goat-anti-mouse immunoglobulins or peroxidase-conjugated mAb anti-HA, respectively. Molecular mass markers are indicated on the left.

Next, the recognition of native CD147 on the HeLa cell surface by soluble lysate of scFv-M6-1B9 was determined using flow cytometric analysis (**Figure 3.12**). As predicted, the soluble scFv-M6-1B9 intrabody could react with CD147 expressed on HeLa cells. However, the signal (MFI) was lower than those obtained from the original antibody, M6-1B9. Contrarily, neither soluble lysate of scFv-SVV3 intrabody nor 293A cell lysate recognized the native CD147 on HeLa cell surface. This strongly suggests that the generated soluble lysate scFv-M6-1B9 from 293A cells carries a CD147-specific paratope which recognizes both recombinant and native CD147.
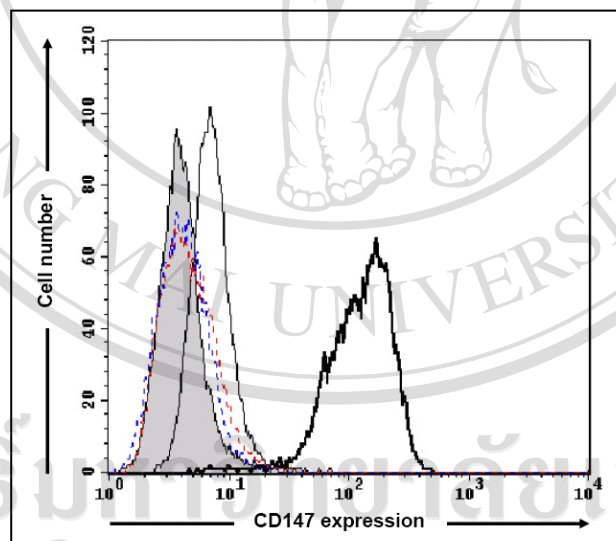
Figure 3.12 The scFv-M6-1B9 intrabody is specific to CD147 on HeLa cell surface. HeLa cell surface staining was performed using soluble lysate of scFv-M6-1B9 intrabody (thin line), scFv-SVV3 intrabody (red dash line), 293A lysate (blue dash line) and M6-1B9 antibody (solid line). Conjugate control was showed in solid shade.

To prove the efficiency of recombinant adenovirus transduction, HeLa (cervical cancer cell), Jurkat (T cell leukemia), U937 (monoblastic cell) and HepG2 (hepatoma cell) were selected as target cells to compare gene transfer efficiency between Ad-scFv-M6-1B9 and Ad5/F35-scFv-M6-1B9. Prior to perform the transduction experiment, all cells were determined the expression of CAR, αv-integrin and CD46. As shown in **Figure 3.13**, U937 and HepG2 cells do not express CAR and αv-integrin. Jurkat cells expressed CAR and αv-integrin at low level. Contrarily, high expression of CAR and αv-integrin was demonstrated in HeLa cells as in control, 293A cells. None of these cell lines express CD46 except HepG2 cells. The cells were subsequently transduced with 0, 100 or 1000 viral particles (VP) per cells. 293A cells were used as control for confirmation the infectivity of both recombinant adenovirus particles. Twenty-four hours after infection the cells were analyzed by flow cytometer for GFP expression. As shown in **Figure 3.14**, Ad5/F35-scFv-M6-1B9 has a significantly higher infectivity than Ad-scFv-M6-1B9 in U937 (60% maximum expression). Due to Ad5/F35-scFv-M6-1B9 used CD46 as a receptor for adenovirus entry, Ad-scFv-M6-1B9 and Ad5/F35-scFv-M6-1B9 had essentially identical and high infectivity for HeLa and Jurkat cells. However, neither Ad-scFv-M6-1B9 nor Ad5/F35-scFv-M6-1B9 could infect HepG2 cells, even at a very high MOI (data not shown).
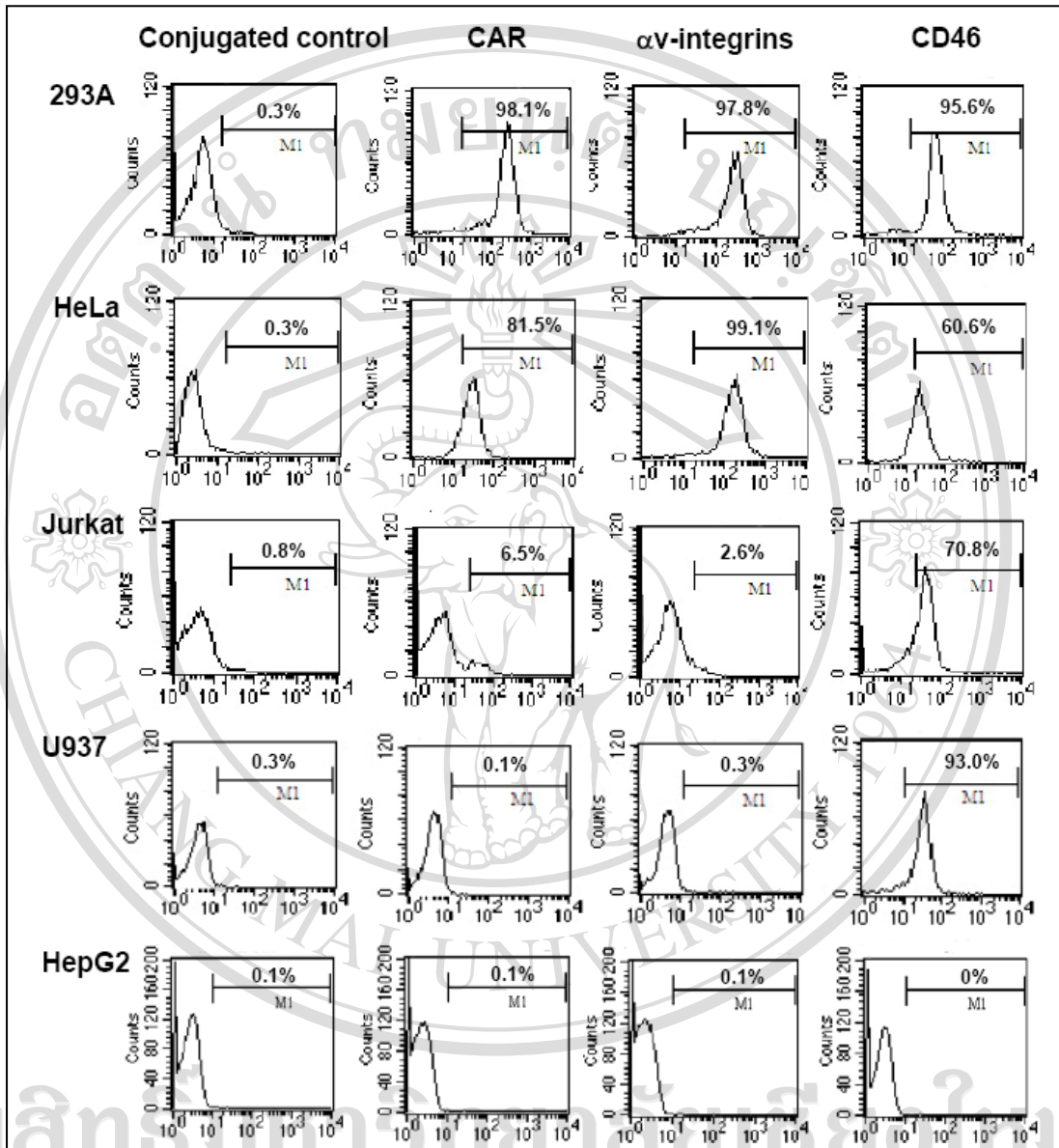
Figure 3.13 Expression of CAR and αv integrin on cell lines. For flow cytometric analysis, 293A, HeLa, Jurkat, U937 and HepG2 cells were incubated with an anti-CAR (RmcB; 1:100 dilution) or anti-αv integrin (L230; 1:100 dilution) mAb or PE-conjugated anti-CD46. The binding of primary antibodies (anti-CAR and anti-αv integrin) was detected by sheep anti-mouse immunoglobulins-PE conjugates (1:100 dilution).
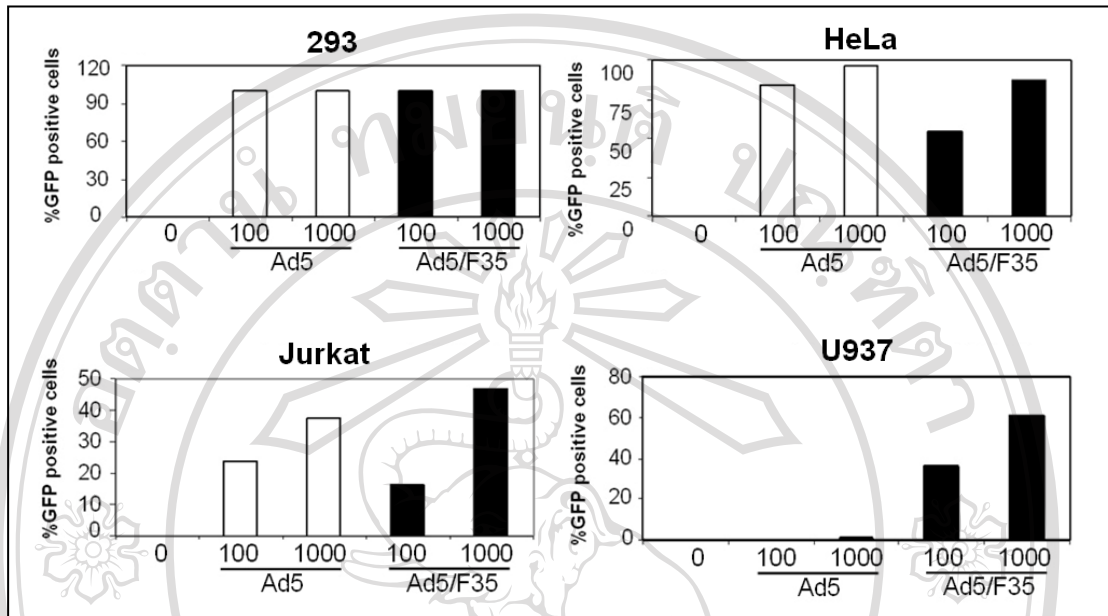
Figure 3.14 Efficient transduction of Ad5 and Ad5/F35 infectivity in four cell lines. Cells were transduced with 0, 100, 1000 viral particles (VP) per cell. After 24 h, the cells were analyzed for GFP expression by flow cytometer. Ad-scFv-M6-1B9 is notated as Ad5 and Ad5/F35-scFv-M6-1B9 as Ad5/F35.

3.8 Intracellular expression of scFv-M6-1B9 intrabody diminished cell surface expression of CD147

3.8.1 293A cells

The compatibility of scFv-M6-1B9 with a eukaryotic expression system was examined by transducing the recombinant adenovirus harboring scFv-M6-1B9 into 293A cells. Alteration of surface expression of CD147 in transduced 293A cells was examined at 36 h after transduction. CD147 cell surface expression was decreased in scFv-M6-1B9 adenovirus-transduced 293A cells compared to untransduced cells (**Figure 3.15**). In contrast, no alteration of CD147 expression was observed on scFv-SVV3 adenovirus transduced cells. This result revealed that intracellular expression of scFv-M6-1B9 as intrabody could diminish CD147 expression on cell surface of intrabody-expressing 293A cells.

Colocalization of scFv-M6-1B9 intrabody and CD147 within 293A cells was elucidated. As shown in **Figure 3.16** and in the three-dimensional movies (**Additional file 1**), scFv-M6-1B9 intrabody was found intracellularly and colocalized with CD147. This result implied that scFv-M6-1B9 protein fused with ER-retention signal was successfully expressed and retained the CD147 molecule inside the cell.
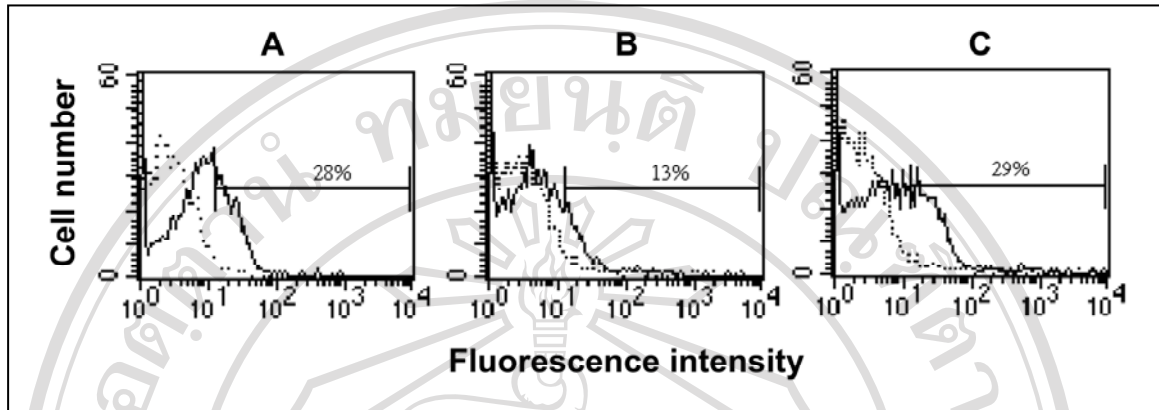
Figure 3.15 Inhibition of CD147 surface expression on 293A cells by M6-1B9 intrabody. 293A cells were transduced with recombinant adenovirus harboring scFv-M6-1B9 or scFv-SVV3. Cell surface staining of CD147 on untransduced **(A)** and scFv-M6-1B9 **(B)** or scFv-SVV3 transduced cells **(C)** was performed using CD147 mAb, M6-1B9 (bold lines) or irrelevant isotype matched mAb (dashed lines). PE-conjugated F(ab')2 fragment of sheep anti-mouse immunoglobulins antibody were used as a secondary antibody. The percentage (%) of CD147 positive cells was indicated.
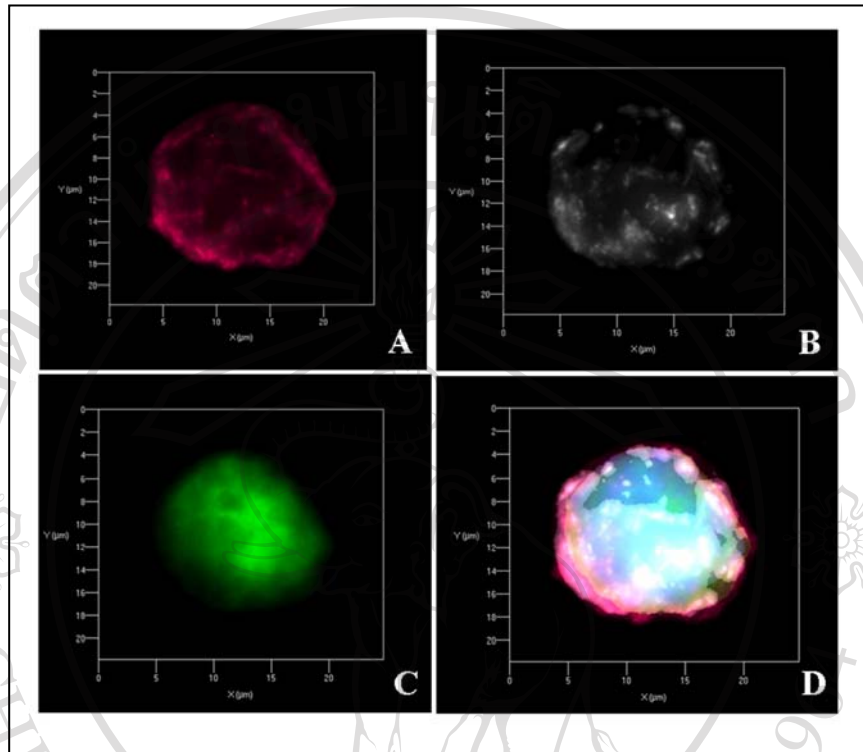
Figure 3.16 Immunocytochemical analysis for colocalization of CD147-intrabody. The transfected 293A cells were fixed and incubated with a mixture of biotinylated anti-human extracellular matrix metalloproteinase inducer (EMMPRIN) mAb and rabbit anti-HA mAb. Then, cells were stained with the mixture of Cy5-conjugated streptavidin and Cy3-conjugated anti-rabbit-IgG mAb. Nuclei were counterstained with DAPI (blue). Three-dimensional (3D) image of the transfected 293A cells was verified. **(A)** CD147 on 293A cell stained with biotinylated anti-human EMMPRIN mAb (red), **(B)** scFv-M6-1B9 intrabody in 293A cell stained with rabbit anti-HA mAb (white), **(C)** GFP positive in transfected cell and **(D)** overlay.

3.8.2 HeLa cells

HeLa cells were used as a representative cancer cell to elucidate the effect of scFv intrabody on the cell surface expression of CD147. HeLa cells were transduced with Ad-scFv-M6-1B9 and Ad-scFv-SVV3 at 200 pfu/cell and analyzed for the surface expression of CD147 at 36 h after transduction. The GFP expression in transduced HeLa cells was demonstrated in **Figure 3.17A.** Nearly 100% of HeLa cells were transduced with Ad-scFv-M6-1B9 and Ad-scFv-SVV3 at MOI of 200. This result indicates that both Ads had essentially identical and high infectivity for HeLa cells. Alteration of surface expression of CD147 in transduced HeLa cells was examined at 36 h after transduction. CD147 cell surface expression was decreased in scFv-M6-1B9 adenovirus-transduced HeLa cells compared to untransduced cells **(Figure 3.17B)**. Interestingly, no alteration of CD147 expression was observed on scFv-SVV3 adenovirus-transduced HeLa cells. The expression of scFv-M6-1B9 intrabody in HeLa cells was analyzed by immunofluorescent staining As shown in **Figure 3.18** and in the three-dimensional movies **(Additional file 2)**, scFv-M6-1B9 intrabody was found intracellularly **(Figure 3.18B)** and colocalized with CD147 **(Figure 3.18D and 3.18E)** . Colocalization between scFv-M6-1B9 intrabody and CD147 was analyzed by FV1000 software. Lambda scan and sequential features were used for separating the cross talk of fluorochromes, Alexa Fluor 488 and Alexa Fluor 568. GFP and Alexa Fluor 488 were separated by spectral unmixing function. The degree of colocalization was quantified using statistical analysis. Pearson's correlation coefficient was 0.51. This result reveals that intracellular expression of scFv-M6-1B9

as intrabody could abate CD147 expression on cell surface of intrabody-expressing
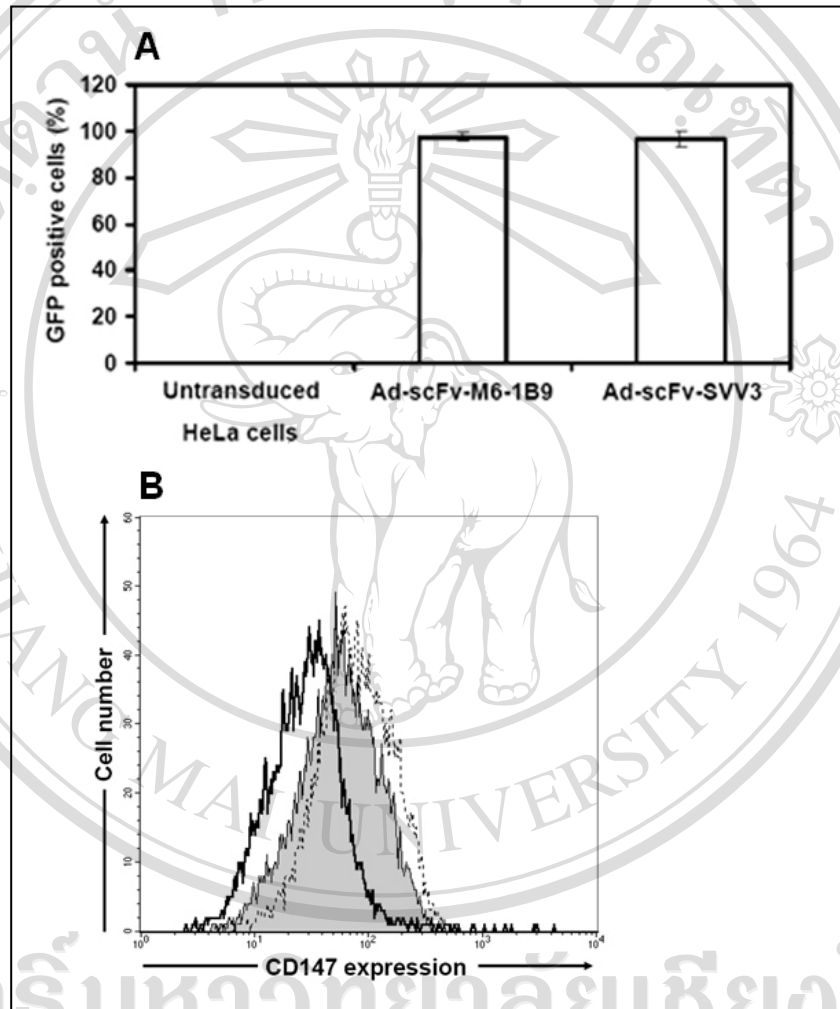
HeLa cells.

Figure 3.17 Inhibition of CD147 surface expression on HeLa cells by M6-1B9 intrabody. **(A)** HeLa cells were transduced with Ad-scFv-M6-1B9 or Ad-scFv-SVV3 at an MOI of 200 pfu/cell. After 36 h, the percentage of GFP-positive cells was determined by flow cytometry. Data represents the average percentage of GFP-expressing cells ± standard error mean (s.e.m.) of three experiments. **(B)** Transduced

HeLa cells with 200 pfu/cell of Ad-scFv-M6-1B9 or Ad-scFv-SVV3 were stained with mouse anti-CD147 mAb (M6-1B9). PE-conjugated F(ab')2 fragment of sheep anti-mouse immunoglobulins antibody were used as a secondary antibody. The fluorescence intensity of CD147 cell surface expression on untransduced HeLa cells (solid shade), transduced cells with Ad-scFv-M6-1B9 (bold line) or Ad-scFv-SVV3 (dash line) is shown. The y axis represents the number of events on a linear scale; the x axis shows the fluorescence intensity on a logarithmic scale.
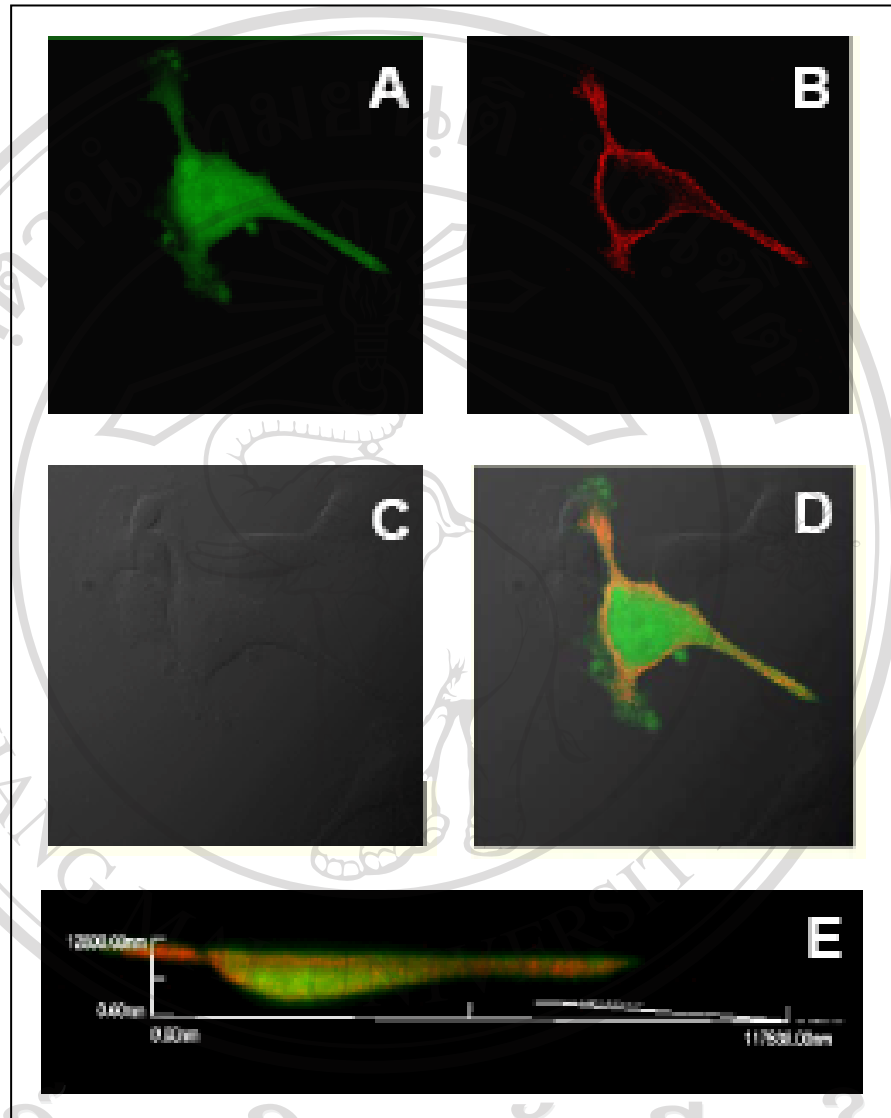
Figure 3.18 Intracellular localization of CD147 in HeLa cells harboring CD147 intrabody. Transduced HeLa cells were seeded on slide chamber, fixed in 4% paraformaldehyde, permeabilized with 0.1% Triton X-100 and stained with a mouse anti-CD147 antibody and a rabbit anti-HA antibody. Secondary detection was performed with Alexa Fluor 488 goat anti–mouse IgG antibody and Alexa Fluor 568 goat anti–rabbit IgG antibody. Images were acquired using an Olympus confocal microscope FV1000. **(A)** CD147 staining with mouse anti-CD147 mAb (green), **(B)**

intrabody scFv M6-1B9 staining with rabbit anti-HA mAb (red), **(C)** phase contrast, **(D)** overlay, colocalization of scFv-M6-1B9 and CD147 (yellowish-orange), and **(E)** three-dimensional (3D) image of the transduced HeLa cells was generated and shown the colocalization of scFv and CD147 (yellowish-orange).
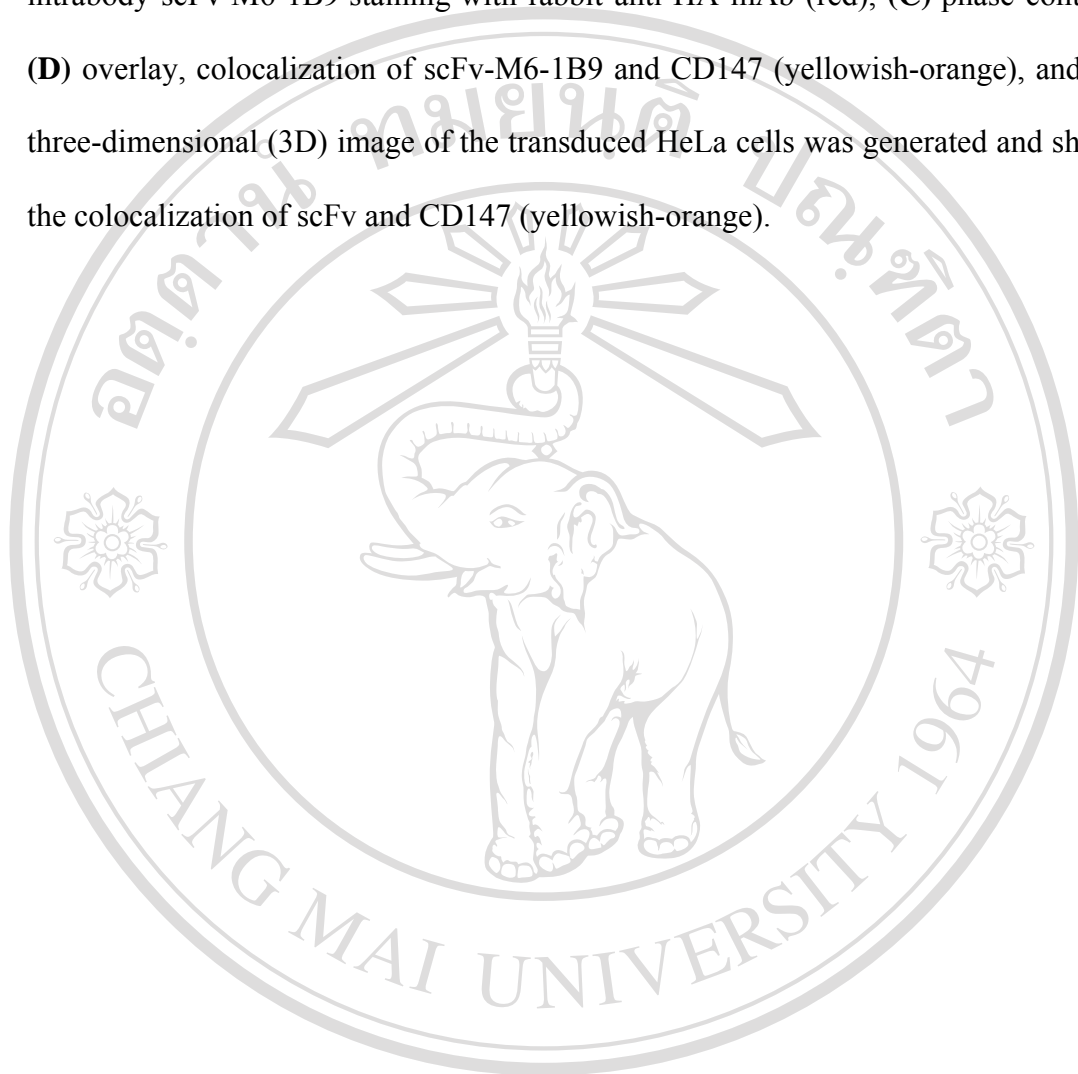
150

3.8.3 Jurkat cells

In general, adenoviral vectors (Ad5) could poorly infect lymphoid leukemic cells. Thus, gene transfer ability of Ad5/F35-scFv-M6-1B9 was further assessed in Jurkat cells. Jurkat cells were transduced with Ad5/F35-scFv-M6-1B9 at various MOI and analyzed for the surface expression of CD147 at 36 h after transduction. The GFP expression in transduced Jurkat cells was demonstrated in **Figure 3.19A.** Fifty percentage of Jurkat cells were transduced with Ad5/F35-scFv-M6-1B9 at MOI of 1. Percentage of GFP-positive cells reached 75% for Jurkat cells transduced by Ad5/F35-scFv-M6-1B9 at an MOI of 100. This result indicates that Ad5/F35-scFv-M6-1B9 had high infectivity for Jurkat cells due to the high expression of CD46 on this cell line (**Figure 3.12**). Alteration of surface expression of CD147 in transduced Jurkat cells was also examined at 36 h after transduction. Interestingly, CD147 cell surface expression was reduced in Ad5/F35-scFv-M6-1B9-transduced Jurkat cells by dose-dependent manner **(Figure 3.19B).**
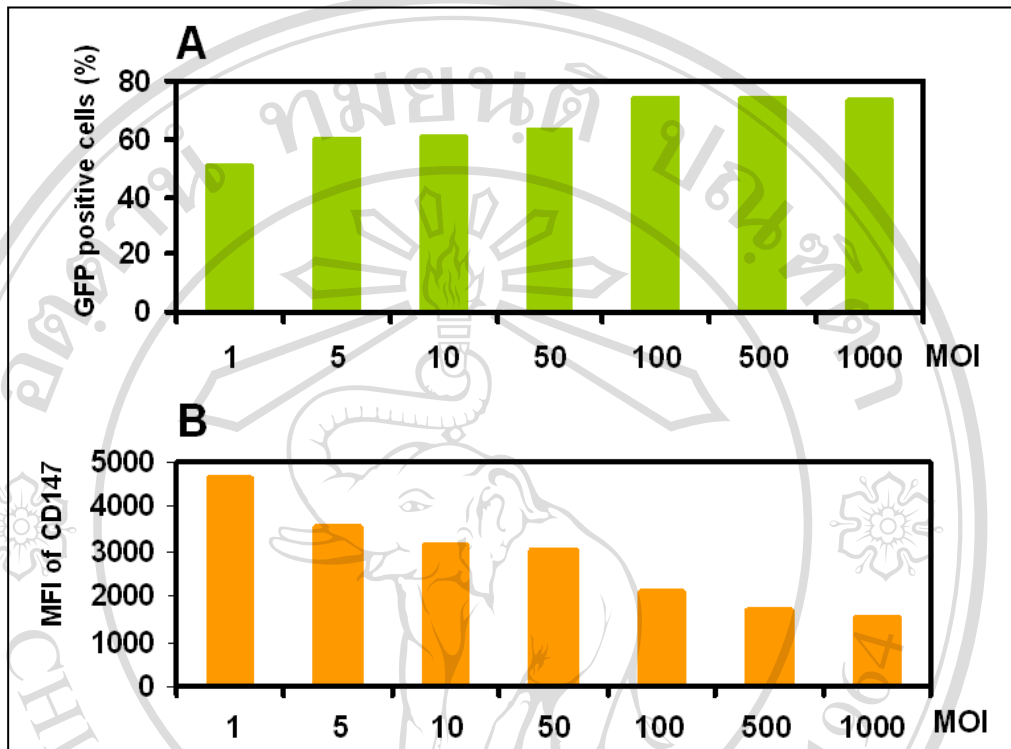
Figure 3.19 Inhibition of CD147 surface expression on Jurkat cells by M6-1B9 intrabody. (**A**) Jurkat cells were transduced with Ad5/F35-scFv-M6-1B9 at various MOI. After 36 h, the percentage of GFP-positive cells was determined by flow cytometry. (**B**) Transduced Jurkat cells with various MOI of Ad5/F35-scFv-M6-1B9 were stained with mouse anti-CD147 mAb (M6-1B9). PE-conjugated F(ab')2 fragment of sheep anti-mouse immunoglobulins antibody were used as a secondary antibody. The *y* axis represents the mean fluorescence intensity (MFI) of CD147 cell surface expression on transduced Jurkat cells; the *x* axis shows the MOI (pfu/cell) of Ad5/F35-scFv-M6-1B9.